Performance and early applications of a versatile double aberration-corrected JEOL-2200FS FEG TEM/STEM at Aalto University

Hua Jiang [a,b,*], Janne Ruokolainen [b], Neil Young [c], Tetsuo Oikawa [d], Albert G. Nasibulin [a], Angus Kirkland [c], Esko I. Kauppinen [a]

[a] *NanoMaterials Group, Department of Applied Physics, Aalto University, Espoo, Finland*
[b] *Nanomicroscopy Center, Aalto University, Espoo, Finland*
[c] *Department of Materials, University of Oxford, Parks Road, Oxford OX1 3PH, UK*
[d] *JEOL (Europe) SAS, Allée de Giverny, 78290 Croissy-sur-Seine, France*

A B S T R A C T

Applications relevant to carbon based nano-materials have been explored using a newly installed JEOL-2200FS field emission gun (FEG) (scanning) transmission electron microscope (S)TEM which is integrated with two CEOS aberration correctors for both the TEM image-forming and the STEM probe-forming lenses. The performance and utility of this newly commission hardware has been reviewed with a particular focus on operation at an acceleration voltage of 80 kV, thus bringing the primary electron beam voltage below the knock-on threshold for carbon materials and opening up a range of possibilities for the study of carbon-based nanostructures in the aberration-corrected electron microscope. The ability of the microscope to obtain both atomic TEM images and high-quality electron diffraction patterns from carbon nanotubes was demonstrated. The chiral structure of a double-walled carbon nanotube was determined from its diffraction pattern. The aberration corrected TEM imaging technique facilitates a unique approach to accurate determination of single-walled carbon nanotube diameters. On the other hand, the probe-corrected high angle annular dark field (HAADF) STEM imaging performance allows for the detection of single gold atoms at 80 kV and was used to study the graphite interlayer spacing in a multi-walled carbon nanotube.

© 2011 Elsevier Ltd. All rights reserved.

1. Introduction

With electron-optical spherical aberration correction technology reaching maturity, a new generation of aberration-corrected electron microscopes has become widespread throughout laboratories concerned with the physical characterization of materials across the world (Smith, 2008). A modern electron microscope can operate either in conventional transmission electron microscope (TEM) mode where a parallel-beam illuminates the specimen, or scanning TEM (STEM) mode where the electron beam is focused to a small probe and scanned across the sample. Correction of electron optical lens aberrations is achievable through application of proprietary 'corrector' hardware for either imaging (TEM) or probe forming (STEM) lenses (Haider et al., 1998b; Batson et al., 2002). Both routinely provide sub-Ångstrom resolution imaging and atomic-level microanalysis (Tanaka, 2008). By incorporating both probe and image aberration correctors and other analytical

instrumentation into a single electron optical column, a double aberration-corrected TEM/STEM has proven a versatile and powerful tool to explore advanced nano-materials on the atomic scale (Hutchison et al., 2005; Kirkland et al., 2008; Zhu and Wall, 2008).
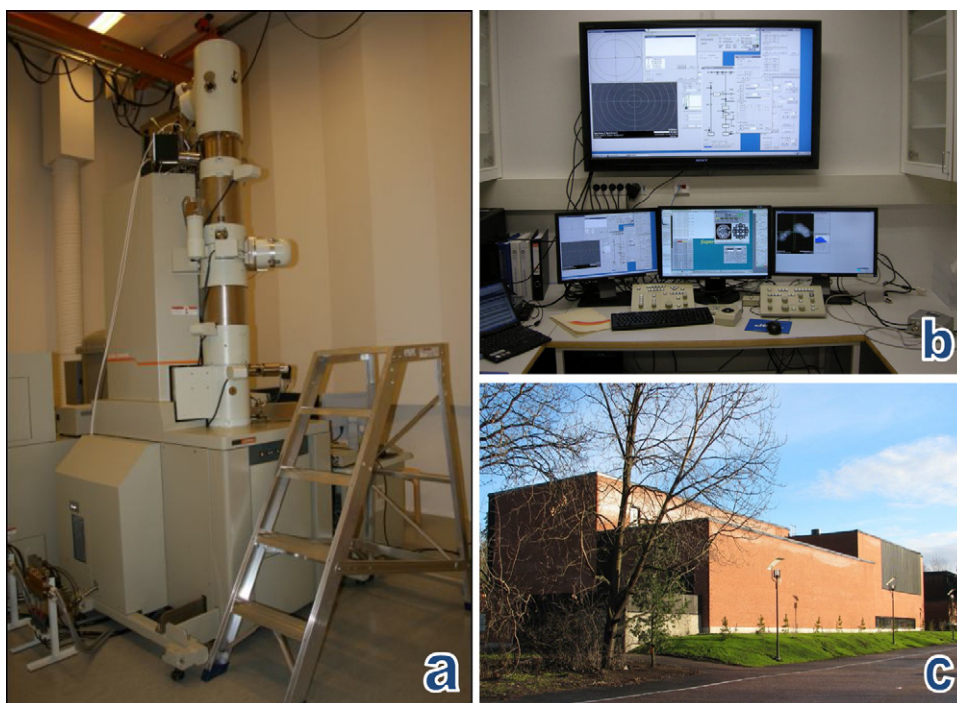
A JEOL-2200FS FEG (S)TEM fitted with hexapole aberration correctors (CEOS GmbH) for both imaging and probe-forming lenses, together with a JEOL in-column omega-type electron energy filter, has recently been installed in a purpose-built building at the Nanomicroscopy Center (NMC) in Aalto University, Finland. The experimental evaluation of similar microscope systems has been reported previously by several pioneer groups (Allard et al., 2004; Blom et al., 2006; Hutchison et al., 2005; Kirkland et al., 2008; Sawada et al., 2005; Zhu and Wall, 2008). In this contribution, our attention is primarily directed towards the evaluation and early applications of our microscope, focusing on its performance at a low operating voltage of 80 kV for the study of carbon based nano-materials.

2. The microscope and its accommodation in brief

Fig. 1 shows the JEOL-2200FS FEG (S)TEM (Fig. 1a) and its remote operation room (Fig. 1b) which are accommodated in a

Fig. 1. (a) A 200 kV Cs-corrected TEM/STEM fitted with both probe forming and imaging correctors; (b) the control panel of the microscope in a remote operating room and (c) a view of the Nanomicroscopy Center at Aalto University.

dedicated building (Fig. 1c) of NMC at Aalto University. The microscope is equipped with a Schottky field emission gun (FEG) and can be operated at accelerating voltages up to 200 kV. It has a JEOL high-resolution pole piece (HRP)-wider gap (4 mm) objective lens to facilitate high experimental flexibility in applications such as electron beam tomography, cryo-TEM, and other dynamic experiments, all performed at high resolution in the aberration-free environment. Two CEOS hexapole-type spherical aberration (Cs-) correctors (Haider et al., 1998a) are seamlessly incorporated into the design of the electron optical column and may be tuned to generate negative Cs, thus compensating for the effects of the positive spherical aberrations inherent in the standard electron objective lens for both TEM and STEM based imaging. The microscope is also fitted with a JEOL lithium–drifted silicon (Si–Li) energy dispersive X-ray spectrometer (EDS) and an in-column Ω-type energy filter facilitating the electron energy loss spectrometry (EELS) and energy filtered TEM (EFTEM). The system is configured for full remote control from a separate operating room (Fig. 1b) in order to minimize human disturbances and to humanize the operation. A Hamamatsu high frame rate digital camera is used for live image viewing and a Gatan 4k × 4k UltraScan 4000 CCD camera is employed for digital recording of TEM images. A high-angle annular dark-field (HAADF) detector above the Ω-filter and a bright-filed (BF) detector under the filter are mounted for digital STEM imaging. A unique piezo-driven stage allows fine control of the specimen position in *x* and *y* directions. The microscope also features an entirely oil-free vacuum system that ensures specimen contamination from any pumping oil in the system is completely eliminated. Furthermore, the microscope operates with full alignments both at 200 kV and at 80 kV.

To guarantee the best performance of such aberration-corrected electron microscopes, the local environment around the microscope must be carefully controlled providing a lowest level of floor vibration, acoustic noise, stray electromagnetic fields, fluctuations in airflow, humidity and room temperature (Allard et al., 2004; Zhu and Wall, 2008). The building of the Nanomicroscopy Center at Aalto University has been designed to minimize external disturbances which might cause interference with the microscopes.
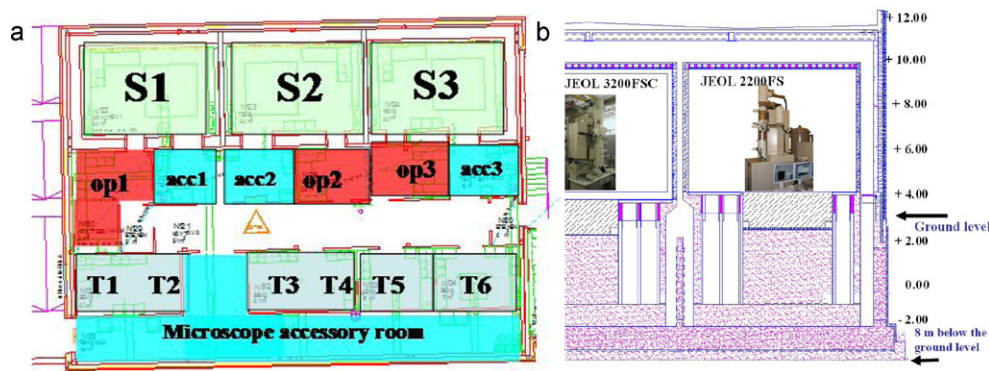
Fig. 2a shows the floor plan of the main instrument section in the NMC building which contains all the microscope rooms (S1–S3 and T1–T6). Other rooms for the main power supply, air handling units and sample preparation are located in a second section (not shown in Fig. 2a) which is physically separated from the main instrument section. The room (S2) that houses the JEOL-2200FS is based on a room-in-room construction, with its column sitting on a fiberglass block of dimensions 3 m × 5 m × 2 m deep, which itself is supported by a 6 m deep concrete block (see Fig. 2b for its cross section profile). The microscope foundation is separated from the rest of the building by two air gaps to prevent outside disturbance. Vertical and horizontal vibrations measured from room S2 are well below 0.1 μm/s, and 0.3 μm/s, respectively, in the low frequency region (<8 Hz), which are generally hard to be damped by the design of the microscope itself. In addition, stray magnetic field measured from all three directions in room S2 with all necessary electronic devices powered on is at a background level around 0.1 nT with the highest peak at about 10 nT, well below JEOL's specification of 100 nT. The fluctuation in room temperature is extremely small, at a rate of approximately ±0.1 °C for months.

3. Performance and applications

The conventional performance tests of the microscope at 200 kV have resulted in comparable performance to those reported earlier by other groups with similarly configured microscopes (Allard et al., 2004; Blom et al., 2006; Hutchison et al., 2005; Kirkland et al., 2008; Sawada et al., 2005). Here we focus our topics on some early results that we have achieved on the microscope operating at 80 kV.

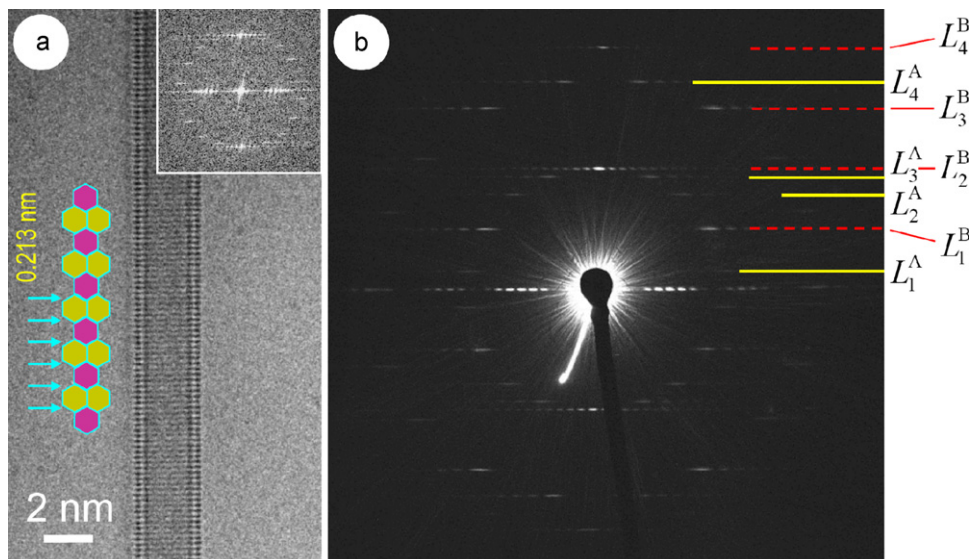### 3.1. TEM imaging and electron diffraction of carbon nanotube at 80 kV

Since their discovery, carbon nanotubes have been extensively studied due to their unique structure and fascinating properties. It is known that the size and chiral angle of a nanotube are two key parameters that determine its properties. High-resolution

Fig. 2. (a) The floor plan of the main section in the NMC building; (b) the cross section profile of the instrument rooms (S1–S3). Architect Ilkka Paajanen, Architect bureau Arto Sipinen and structural design Raimo Salminen, Magnus Malmberg Consulting Engineers.
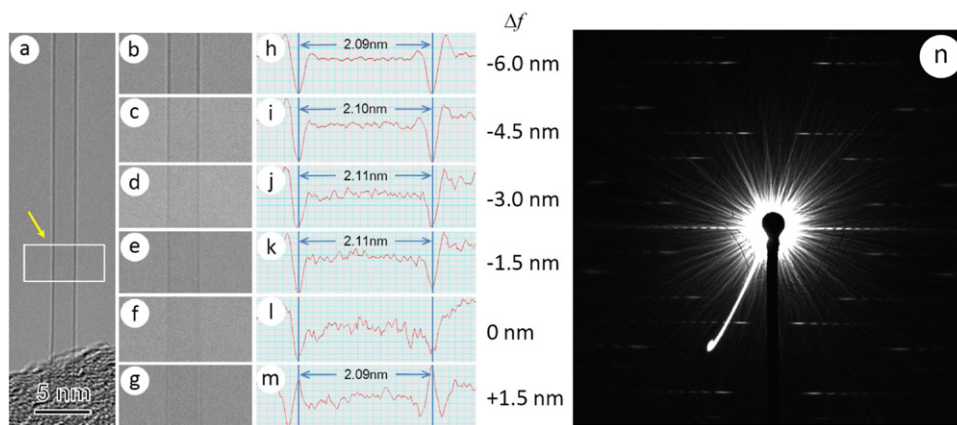
transmission electron microscopy (HRTEM) has been one of the most widely used tools for structural characterization of carbon nanotubes. A single walled carbon nanotube (SWCNT) usually appears in a conventional TEM image as simply a pair of parallel dark fringes which are regarded as two edges of the nanotube. For a double-walled carbon nanotube (DWCNT), four separate walls appear as two pairs of dark lines. It is not until recently that the ease of using the aberration-corrected TEM enables atomic imaging of SWCNTs, from which direct structure determination is possible (Hashimoto et al., 2004; Hirahara et al., 2006; Warner et al., 2009) but usually challenging with some inherent ambiguity due to the typical weak contrast and low signal-to-noise level. It is even worse for a DWCNT, where two tubes are usually incommensurate and the projection of four curved graphitic layers generates complex Moiré patterns (Zuo et al., 2003). In contrast, electron diffraction has been proven powerful in structure evaluation of carbon nanotubes (Gao et al., 2003; Jiang et al., 2007; Kociak et al., 2002). Here we demonstrate the ability of using the JEOL-2200FS microscope to form atomic resolution images and to obtain high-quality electron diffraction patterns from carbon nanotubes at a low operating voltage of 80 kV, which is considered to avoid severe electron beam induced knock-on damage in carbon nanotubes. (Zobelli et al., 2007). As an example, an 80 kV aberration-corrected high resolution TEM lattice image of a DWCNT is shown in Fig. 3a, and a

corresponding electron diffraction pattern is presented in Fig. 3b. In the TEM image, the Moiré pattern is clearly visible between two intense dark lines. The FFT pattern (inset) of the image displays a number of discrete layer lines. However, the definition of both the image and its FFT pattern are insufficient for unambiguous determination of the atomic structure of the nanotubes. Fortunately, the electron diffraction pattern shown in Fig. 3b, which also features many discrete layer lines, is nearly perfectly defined in terms of layer lines' positions and intensity distributions. Careful layer line distance analysis (Jiang et al., 2008) indicates that, in the upper half of the pattern, four yellow solid lines originate from diffraction of one nanotube (Tube A), while four other (red dashed) lines which are equally spaced correspond to the other nanotube (Tube B). Further analysis of the layer line intensity profile on the base of a robust Bessel-function-based method (Jiang et al., 2006) identifies the order of Bessel function for each individual layer line. As a result, Bessel function orders of two independent layer lines L_2^A and L_3^A for Tube A are determined to be 17 and 10, giving the chiral indices of Tube A as (17, 10). For Tube B, two independent layer lines L_1^B and L_2^B are recognized having Bessel function orders as 32 and 0, respectively, thus Tube B is a zigzag tube indexed as (32, 0). The chiral angles of Tube A and Tube B are 21.49° and 0°, and the diameters of the two nanotubes are 1.85 nm and 2.51 nm, respectively. Apparently, we see that Tube A is the inner tube and Tube B

Fig. 3. (a) An 80 kV aberration-corrected TEM lattice image of a double-walled carbon nanotubes with its FFT pattern as an inset. The C–C zigzag chains in the outer zigzag nanotube is schematically indicated with arrows. (b) The corresponding electron diffraction pattern of the DWCNT.

Fig. 4. (a) An aberration-corrected HREM image of a SWCNT; (b–g) a through-focal series of images corresponding to the framed region indicated by the arrow in (a); (h–m) line profiles plotted from the related images indicating the spacing of the two prime fringes in the images. The nominal instrument focus values (Δf) are given in the right column. (n) The electron diffraction pattern of the investigated SWCNT, from which the chirality of the nanotube is determined to be (22, 8).

is the outer tube, and the interlayer distance between two walls of the nanotubes is calculated as 0.33 nm. With the carbon nanotube structure determined, it is understandable that the TEM image contrast of the investigated DWCNT is dominated by the modulation due to the C–C zigzag chains (Hashimoto et al., 2004) in the outer (32, 0) zigzag tube (indicated schematically by arrows in Fig. 3a) which is lined up in a repeating period of 0.213 nm along the axial direction of the nanotube.

3.2. Accurate measurement of carbon nanotube diameters from aberration-corrected TEM images

Successful applications of single-walled carbon nanotubes relies largely on accurate determination of their structural parameters. It is broadly recognized that the diameter of a carbon nanotube can be measured on its HRTEM images by measuring the spacing of two related parallel dark fringes. However, the image contrast of a SWCNT depends strongly on imaging conditions as well as the spherical aberration coefficient of the microscope. It was claimed that the diameter of a SWCNT can hardly be measured accurately from conventional HRTEM images (Qin and Peng, 2002). However, aberration correction techniques in electron optical system have led to dramatically increased resolution, sensitivity and signal to noise in high-resolution microscopy, thus, opening a new approach to the imaging of SWCNTs with high precision.
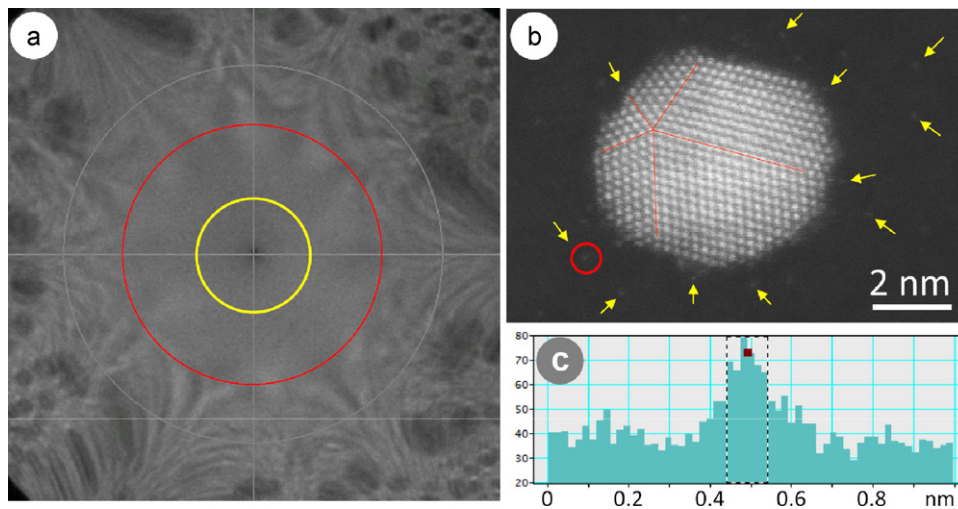
Fig. 4a shows an aberration corrected HRTEM image of a SWCNT which was taken with the microscope at 80 kV. The image displays a pair of parallel dark fringes surrounded by white fringes. To evaluate the dependence of the image contrast on the focusing condition, a through-focal series of images was recorded with a focal step of 1.5 nm. Fig. 4b–g shows images of the same portion of the nanotube (the framed region indicated by an arrow in Fig. 4a at nominal instrument focus values (Δf) and Fig. 1h–m shows line profiles plotted from the corresponding images. Image analysis indicated that, with the aberration corrected TEM, the measurements of the spacing between the two dark fringes changed little with the focus condition except for $\Delta f \geq 0$ nm where the dimension is not well defined. The measurement error induced by changing Δf from −1.5 nm to −6.0 nm is less than 1%. To correlate the measurement of the dark fringe spacing to the actual nanotube diameter, an electron diffraction pattern (EDP) shown in Fig. 4n was taken from the nanotube on the same microscope at 80 kV. By using a unique calibration-free method based on intrinsic layer line distance analysis of the EDP (Jiang et al., 2007), the chirality of the SWCNT was determined to be (22, 8), thus the nanotube diameter is 2.11 nm.

With this value, the microscope can now be calibrated at a certain focusing condition, e.g. $\Delta f = −1.5$ nm, thereafter, the microscope is capable of measuring the nanotube diameter with high accuracy.

3.3. HAADF-STEM imaging at 80 kV

High angle annular dark field (HAADF) STEM imaging is well suited to the observation of heavy metal atom clusters on amorphous supporting films of low atomic number materials (Nellist and Pennycook, 1996; Young et al., 2008). Single atom detection using the HAADF-STEM technique at 200 kV has been previously reported (Blom et al., 2006; Tanaka, 2008), and atomic level structural and chemical analysis is now becoming routine at lower acceleration voltages (Krivanek et al., 2010). In our test, nano-sized Au clusters on an amorphous carbon film were used. The Cs-corrected STEM performance at 80 kV was firstly evaluated by using the electron Ronchigram of an amorphous carbon film as a diagnostic tool for the residual lens aberrations (Lin and Cowley, 1986). Fig. 5a shows that the coherent flat phase region of the focused electron Ronchigram was observed up to 30 mrad semiangle. A condenser lens aperture of a radius about 20 mrad (indicated by the inner yellow circle in Fig. 5a) was used while a HAADF image was scanned. Fig. 5b is an HAADF STEM image of a fivefold axis decahedral Au nano-crystal surrounded by a number of separated white dots which are believed to be single gold atoms (indicated by arrows). The intensity profile crossing one of those spots (circled in Fig. 5b) with a well-defined shape is shown in Fig. 5c, giving the full width at half maximum (FWHM) about 0.101 nm.

Following this successful test we applied the HAADF-STEM imaging technique to observe multi-walled carbon nanotubes (MWCNTs) which has relatively low contrast compared to heavy metal materials. Shown in Fig. 4a and b are a pair of STEM images of a MWCNT sample (at 80 kV) which were acquired on the bright-field (BF) detector and subsequently on the HAADF detector. BF-STEM images are largely produced by coherent elastic scattering and collected over a range of collection angles very close to the optical axis. Therefore they exhibit many of the phase-contrast image properties of a conventional bright-field TEM image. Fig. 6a presents a high-resolution BF- STEM lattice fringe image of the carbon nanotube, showing fine structures of dotted features along the nanotube walls, which typically arise from the coherent interference between different Bragg beams. On the contrary, the incoherent HAADF image (Fig. 6b) shows just the bright line features with typical graphite interlayer spacing of 0.34 nm. It is noted that carbon nanotubes are not suitable for testing the HAADF image resolution due to their lack of high-angle thermal diffuse scattering for HAADF collection.
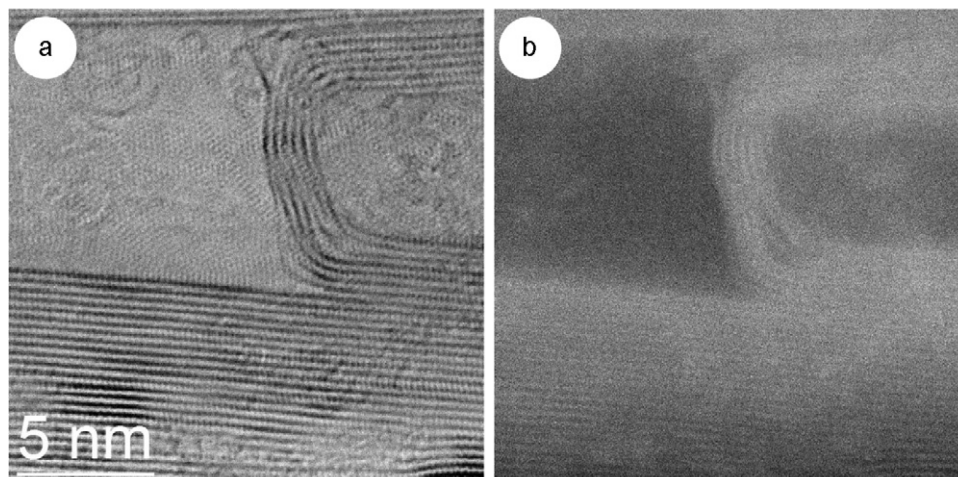
Fig. 5. (a) Electron Ronchigram of the Cs-corrected electron probe focused on a thin amorphous carbon film. The coherent flat phase region (red circle) was observed up to 30 mrad semiangle. HAADF images were scanned by using a condenser lens aperture of a radius about 20 mrad (yellow circle) (b) an HAADF STEM image of a fivefold axis decahedral Au nano-crystal surrounded by a number of single Au atoms; and (c) an intensity profile crossing the circled atom in (b). (For interpretation of the references to color in this figure legend, the reader is referred to the web version of the article.)

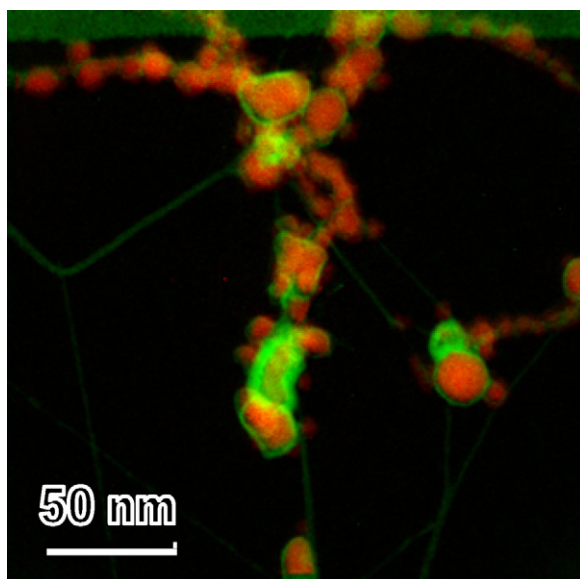### 3.4. Electron energy-filtered TEM (EFTEM) imaging of carbon nanotubes

The Ω-type energy filter installed in the microscope allows acquisition of elastic zero-loss electronic images (or diffraction patterns) and elemental maps of thin specimens using inelastically scattered electrons in addition to EELS analysis. EFTEM with an in-column electron energy filter is as simple to operate as the conventional TEM due to the unique symmetrical design of the spectrometer, which compensates automatically for image distortion in the achromatic image plane. The 4k × 4k CCD camera is effective to provide enough pixel resolution though being binned up to 8× under low signal conditions to increase the SNR. Fig. 7 gives an example of the energy-filtered elemental mapping (at 80 kV) of a single-walled carbon nanotube (SWCNT) sample which was synthesized in a gas-phase floating catalyst CVD reactor (Anisimov et al., 2010) where iron nanoparticles derived from ferrocene vapor decomposition act as catalysts. The sharp elemental map clearly reveals the carbon distribution, especially its thin coating layer around the Fe catalysts, which helps understanding the growth mechanism of carbon nanotubes.

4. Summary

A double-aberration corrected and energy-filtered analytical JEOL-2200FS TEM/STEM has recently been installed at Aalto University, in a dedicated building that provides an exceptionally stable environment for high-resolution electron microscopy. In addition to its reputable performance at 200 kV, the microscope has been demonstrated to show excellent performance at 80 kV with versatility. Both atomic TEM imaging and high-quality electron diffraction have been proven practical on carbon nanotube structure determination. Aberration-corrected HAADF-STEM image of gold atoms embedded in an amorphous carbon film demonstrates the ability of the microscope for single atom detection. The graphite interlayer spacing in a multi-walled carbon nanotube is resolved in its HAADF image. With the aid of the aberration correction technique, a feasible method has been set up for accurate measurement of single-walled carbon nanotube diameters. The microscope operating at 80 kV makes it suitable for investigation of beam sensitive materials like carbon based nanomaterials that suffer easily from knock-on damage.

Fig. 6. A Cs-corrected STEM bright-field image (a), and a corresponding Cs-corrected STEM dark-field image (b) of a multi-walled carbon nanotube.

Fig. 7. An energy-filtered elemental mapping (at 80 kV) of a single-walled carbon nanotube sample showing clear elemental distribution of both C (green) and Fe (red). (For interpretation of the references to color in this figure legend, the reader is referred to the web version of the article.)

Acknowledgments

References

Allard, L.F., Blom, D.A., O'Keefe, M.A., Kiely, C., Ackland, D., Watanabe, M., Kawasaki, M., Kaneyama, T., Sawada, H., 2004. First results from the aberration-corrected JEOL 2200FS-AC STEM/TEM. Microscopy and Microanalysis 10, 110–111.

Anisimov, A.S., Nasibulin, A.G., Jiang, H., Launois, P., Cambedouzou, J., Shandakov, S.D., Kauppinen, E.I., 2010. Mechanistic investigations of single-walled carbon nanotube synthesis by ferrocene vapor decomposition in carbon monoxide. Carbon 48, 380–388.

Batson, P.E., Dellby, N., Krivanek, O.L., 2002. Sub-Ångstrom resolution using aberration corrected electron optics. Nature 418, 617–620.

Blom, D.A., Allard, L.F., Mishina, S., O'Keefe, M.A., 2006. Early results from an aberration-corrected JEOL 2200FS STEM/TEM at Oak Ridge National Laboratory. Microscopy and Microanalysis 12, 483–491.

Gao, M., Zuo, J.M., Twesten, R.D., Petrov, I., Nagahara, L.A., Zhang, R., 2003. Structure determination of individual single-wall carbon nanotubes by nanoarea electron diffraction. Applied Physics Letters 82, 2703–2705.

Haider, M., Rose, H., Uhlemann, S., Schwan, E., Kabius, B., Urban, K., 1998a. A spherical-aberration-corrected 200 kV transmission electron microscope. Ultramicroscopy 75, 53–60.

Haider, M., Uhlemann, S., Schwan, E., Rose, G., Kabius, B., Urban, K., 1998b. Electron microscopy image enhanced. Nature 392, 768–769.

Hashimoto, A., Suenaga, K., Gloter, A., Urita, K., Iijima, S., 2004. Direct evidence for atomic defects in graphene layers. Nature 430, 870–873.

Hirahara, K., Saitoh, K., Yamasaki, J., Tanaka, N., 2006. Direct observation of six-membered rings in the upper and lower walls of a single-wall carbon nanotube by spherical aberration-corrected HRTEM. Nano Letters 6, 1778–1783.

Hutchison, J.L., Titchmarsh, J.M., Cockayne, D.J.H., Doole, R.C., Hetherington, C.J.D., Kirkland, A.I., Sawada, H., 2005. A versatile double aberration-corrected, energy filtered HREM/STEM for materials science. Ultramicroscopy 103, 7–15.

Jiang, H., Brown, D.P., Nasibulin, A.G., Kauppinen, E.I., 2006. Robust Bessel-function-based method for determination of the (n,m) indices of single-walled carbon nanotubes by electron diffraction. Physical Review B – Condensed Matter and Materials Physics 74, 035427.

Jiang, H., Brown, D.P., Nikolaev, P., Nasibulin, A.G., Kauppinen, E.I., 2008. Determination of helicities in unidirectional assemblies of graphitic or graphiticlike tubular structures. Applied Physics Letters 93, 141903.

Jiang, H., Nasibulin, A.G., Brown, D.P., Kauppinen, E.I., 2007. Unambiguous atomic structural determination of single-walled carbon nanotubes by electron diffraction. Carbon 45, 662–667.

Kirkland, A., Chang, L.Y., Haigh, S., Hetherington, C., 2008. Transmission electron microscopy without aberrations: applications to materials science. Current Applied Physics 8, 425–428.

Kociak, M., Suenaga, K., Hirahara, K., Saito, Y., Nakahira, T., Iijima, S., 2002. Linking chiral indices and transport properties of double-walled carbon nanotubes. Physical Review Letters 89, 155501–155504.

Krivanek, O.L., Chisholm, M.F., Nicolosi, V., Pennycook, T.J., Corbin, G.J., Dellby, N., Murfitt, M.F., Own, C.S., Szilagyi, Z.S., Oxley, M.P., Pantelides, S.T., Pennycook, S.J., 2010. Atom-by-atom structural and chemical analysis by annular dark-field electron microscopy. Nature 464, 571–574.

Lin, J.A., Cowley, J.M., 1986. Calibration of the operating parameters for an HB5 stem instrument. Ultramicroscopy 19, 31–42.

Nellist, P.D., Pennycook, S.J., 1996. Direct imaging of the atomic configuration of ultradispersed catalysts. Science 274, 413–415.

Qin, C., Peng, L.M., 2002. Measurement accuracy of the diameter of a carbon nanotube from TEM images. Physical Review B – Condensed Matter and Materials Physics 65, 1554311–1554317.

Sawada, H., Tomita, T., Naruse, M., Honda, T., Hambridge, P., Hartel, P., Haider, M., Hetherington, C., Doole, R., Kirkland, A., Hutchison, J., Titchmarsh, J., Cockayne, D., 2005. Experimental evaluation of a spherical aberration-corrected TEM and STEM. Journal of Electron Microscopy 54, 119–121.

Smith, D.J., 2008. Progress and perspectives for atomic-resolution electron microscopy. Ultramicroscopy 108, 159–166.

Tanaka, N., 2008. Present status and future prospects of spherical aberration corrected TEM/STEM for study of nanomaterials. Science and Technology of Advanced Materials 9, 014111.

Warner, J.H., Schäffel, F., Zhong, G., Rümmeli, M.H., Büchner, B., Robertson, J., Briggs, G.A.D., 2009. Investigating the diameter-dependent stability of single-walled carbon nanotubes. ACS Nano 3, 1557–1563.

Young, N.P., Li, Z.Y., Chen, Y., Palomba, S., Di Vece, M., Palmer, R.E., 2008. Weighing supported nanoparticles: size-selected clusters as mass standards in nanometrology. Physical Review Letters 101, 246103.

Zhu, Y., Wall, J., 2008. Chapter 12 Aberration-corrected electron microscopes at Brookhaven National Laboratory. Advances in Imaging and Electron Physics, 481–523.

Zobelli, A., Gloter, A., Ewels, C.P., Seifert, G., Colliex, C., 2007. Electron knock-on cross section of carbon and boron nitride nanotubes. Physical Review B – Condensed Matter and Materials Physics 7, 5.

Zuo, J.M., Vartanyants, I., Gao, M., Zhang, R., Nagahara, L.A., 2003. Atomic resolution imaging of a carbon nanotube from diffraction intensities. Science 300, 1419–1421.